Universal density of low-frequency states in silica glass at finite temperatures

Roberto Guerra,[1] Silvia Bonfanti,[1] Itamar Procaccia,[2,3] and Stefano Zapperi[1,4]

[1]*Center for Complexity and Biosystems, Department of Physics, University of Milan, via Celoria 16, 20133 Milano, Italy*
[2]*Department of Chemical Physics, The Weizmann Institute of Science, Rehovot 76100, Israel*
[3]*Center for OPTical IMagery Analysis and Learning, Northwestern Polytechnical University, Xi'an, 710072 China*
[4]*CNR-Consiglio Nazionale delle Ricerche, Istituto di Chimica della Materia Condensata e di Tecnologie per l'Energia, Via R. Cozzi 53, 20125 Milano, Italy*

(Received 20 September 2021; accepted 13 April 2022; published 3 May 2022)

The theoretical understanding of the low-frequency modes in amorphous solids at finite temperature is still incomplete. The study of the relevant modes is obscured by the dressing of interparticle forces by collision-induced momentum transfer that is unavoidable at finite temperatures. Recently, it was proposed that low-frequency modes of vibrations around the *thermally averaged* configurations deserve special attention. In simple model glasses with bare binary interactions, these included quasilocalized modes whose density of states appears to be universal, depending on the frequencies as $D(\omega) \sim \omega^4$, in agreement with the similar law that is obtained with bare forces at zero temperature. In this paper, we report investigations of a model of silica glass at finite temperature; here the bare forces include binary and ternary interactions. Nevertheless, we can establish the validity of the universal law of the density of quasilocalized modes also in this richer and more realistic model glass.

DOI: 10.1103/PhysRevE.105.054104

I. INTRODUCTION

Simple models of amorphous solids employ ensembles of particles interacting via binary forces [1]. Choosing different sizes of particles (or, equivalently, ranges of interaction of these forces), one can create useful models of glass forming systems. In athermal conditions ($T = 0$), these given forces offer also a straightforward path to analyzing the vibrational modes around a local energy minimum state [2]. The bare Hamiltonian $U(\boldsymbol{r}_1, \ldots \boldsymbol{r}_N)$ provides the Hessian (or force-constant) matrix $\boldsymbol{H}$ which determines, in the harmonic approximation, all the modes and their frequencies [3],

$$H_{ij}^{\alpha\beta} \equiv \frac{1}{\sqrt{m_i m_j}} \frac{\partial^2 U(\boldsymbol{r}_1, \ldots \boldsymbol{r}_N)}{\partial r_i^\alpha \partial r_j^\beta}. \tag{1}$$

Here $\boldsymbol{r}_i$ is the ith coordinate of a constituent atom of mass m_i in a system with N atoms. As long as the $T = 0$ configuration is stable, all the eigenvalues of the bare Hessian are real and positive (with the exception of few possible zeros associated with Goldstone modes). The force on each atom $\boldsymbol{F}_i$ is given by $-\partial U(\boldsymbol{r}_1, \ldots \boldsymbol{r}_N)/\partial \boldsymbol{r}_i$, and it vanishes for all i's in athermal equilibrium. One then computes the eigenfunctions and eigenvalues of the Hessian $\boldsymbol{H}$. The eigenvalues λ_i are related to the frequency ω_i according to

$$\omega_i = \pm\sqrt{\lambda_i}. \tag{2}$$

In amorphous solids, the eigenfunctions can be extended or quasilocalized with possible hybridization between these classes. In principle, one can distinguish between these different types of modes by considering the participation ratio (PR) which is defined as in previous papers [4],

$$\mathrm{PR} = \left[N \sum_i (\boldsymbol{e}_i \cdot \boldsymbol{e}_i)^2 \right]^{-1}, \tag{3}$$

where $\boldsymbol{e}_i$ is the ith element of a given eigenfunction of the Hessian matrix. We expect the participation ratio to be of order $O(1/N)$ for a quasilocalized mode (QLM) and of order unity for an extended mode. It was expected for a long time [5–8] that the QLMs display a density of states (DOS) $D(\omega)$ with a universal power law,

$$D(\omega) \sim \omega^4 \quad \text{in all dimensions.} \tag{4}$$

However, the actual verification of this prediction was slow in coming. The difficulty is that in large systems the QLMs hybridize strongly with low-frequency delocalized elastic extended modes. The latter are expected to follow the Debye theory with density of states depending on frequency as ω^{d-1} where d is the spatial dimension. Recently, a remedy was found: By examining *small* systems one can bound the frequency of Debye modes from below, exposing the low-frequency QLMs to shine in isolation [9]. Indeed, in such circumstances the universal law Eq. (4) can easily be demonstrated. A direct verification of such a law with numerical simulations of glass formers with binary interactions [10–15] and for silica glass with binary and ternary interactions [4,16] was recently achieved.

Once we turn to finite temperatures, however, it is not immediately obvious how to examine the existence of a similar universal law. The system is never at rest with atoms moving, colliding, and imparting momentum. The bare Hessian matrix

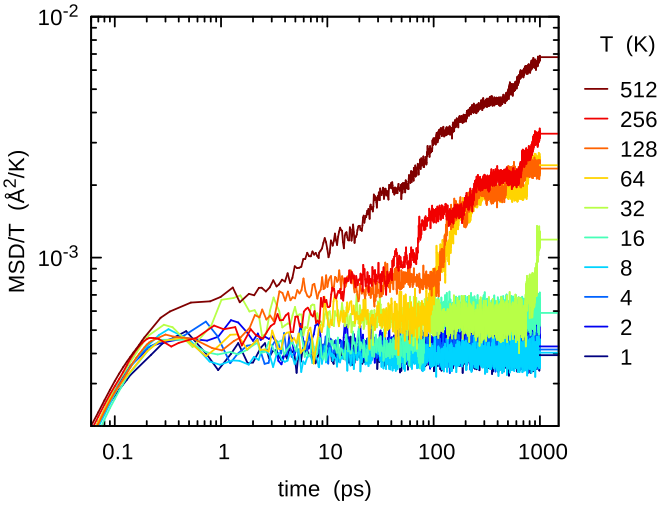

FIG. 1. Starting from the inherent structure configuration, we perform molecular dynamics monitoring the mean squared displacement. Here we plot mean square displacements (MSDs) vs time. In the considered time window at a large-enough T the cages break and the MSD deviates from the plateau. The final horizontal lines were added to report the final average value of each curve.

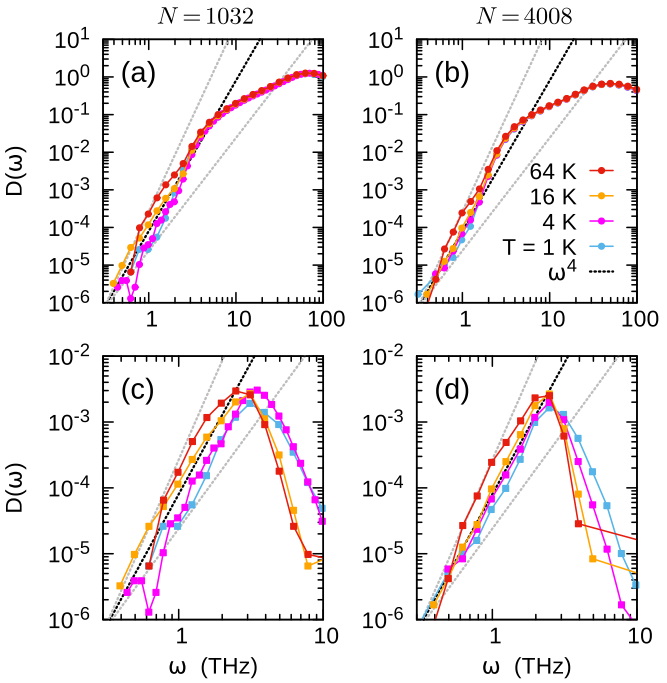

FIG. 2. Density of states as computed from the effective Hessian at different temperatures, $T = 1, 4, 16, 64$ K for SiO_2 glass samples of 1032 [panels (a) and (c)] and 4008 [panels (b) and (d)] atoms. In panels (a) and (b) all the eigenfrequencies are included whereas in panels (c) and (d) only the modes with participation ratios smaller than 0.1 are considered. For all T values, data from over 1000 samples were included. The gray dotted lines report the ω^3 and ω^5 trends.

Eq. (1) loses its usefulness since it generically gains negative eigenvalues when computed in a given frozen configuration. The total force $\boldsymbol{F}_i$ on an ith atom as computed from the bare Hamiltonian, does not vanish, and the eigenfunctions of the bare Hessian lose their meaning as modes associated with a frequency of vibration around a well defined energy minimum. We, thus, need a new definition of modes that mimics their athermal counterparts.

A recently proposed idea focuses on the thermal *average* positions of our atoms and the modes of fluctuations around these [17,18]. The average positions of a thermal glass are constant on timescales shorter than the typical diffusion time τ_G. We, thus, need to consider relatively stable glasses at sufficiently low temperatures such that the cage structure around every atom remains stable, apart from thermal motion for times that are sufficiently long to allow the evaluation of the average position of each atom but sufficiently shorter than the diffusion time at which the cage structure is destroyed. At these average positions, the bare forces do not vanish, but one can consider effective forces which are derived from an effective Hamiltonian that takes into account the dressing of the forces due to the momentum transfer during collisions. Of course, these forces will no longer be binary, but rather have ternary, quaternary, and higher order contributions [19,20]. Whereas it is quite hard to determine precisely the effective forces, it is rather straightforward to define the effective Hessian. To this end, we compute the time averaged positions $\boldsymbol{R}_i$,

$$\boldsymbol{R}_i \equiv \frac{1}{\tau}\int_0^\tau dt\, \boldsymbol{r}_i(t), \tag{5}$$

where $\tau \ll \tau_G$. By definition, the positions $\boldsymbol{R}_i$ are time independent and the configuration $\{\boldsymbol{R}_i\}_{i=1}^N$ is stable, at least, within the time interval $[0, \tau_G]$. An additional quantity of importance is the covariance matrix $\boldsymbol{\Sigma}$, defined as

$$\boldsymbol{\Sigma}_{ij} \equiv \frac{\sqrt{m_i m_j}}{\tau}\int_0^\tau dt[\boldsymbol{r}_i(t) - \boldsymbol{R}_i][\boldsymbol{r}_j(t) - \boldsymbol{R}_j]. \tag{6}$$

We can now define an effective Hessian via

$$\mathbf{H}^{(\mathrm{eff})} = k_B T\, \boldsymbol{\Sigma}^{+}. \tag{7}$$

Here $\boldsymbol{\Sigma}^{+}$ is the pseudoinverse of the covariance matrix [17]. Next, we note that the effective Hessian given by Eq. (7) and the covariance matrix have the same set of eigenfunctions,

$$\mathbf{H}^{(\mathrm{eff})}\boldsymbol{\Psi}_i = \lambda_i^H \boldsymbol{\Psi}_i, \tag{8}$$

and their eigenvalues are related by

$$\lambda_i^H = \frac{k_B T}{\lambda_i^\Sigma}. \tag{9}$$

For all the calculations we have computed the eigenvalues λ_i^H from the covariance matrix by taking the inverse of its eigenvalues λ_i^Σ using Eq. (9), after removing the Goldstone modes. In Ref. [17], it was shown that the eigenvalues and eigenfunctions of $\mathbf{H}^{(\mathrm{eff})}$ serve the same role for the time-averaged configuration as the corresponding ones for the bare Hessian play for the athermal configuration. Indeed, in simple model glass formers one could show that the QLMs of $\mathbf{H}^{(\mathrm{eff})}$ have a universal density of states of the form of Eq. (4). The aim of this paper is to examine how universal this result is by studying in silica glass at nonvanishing temperatures.

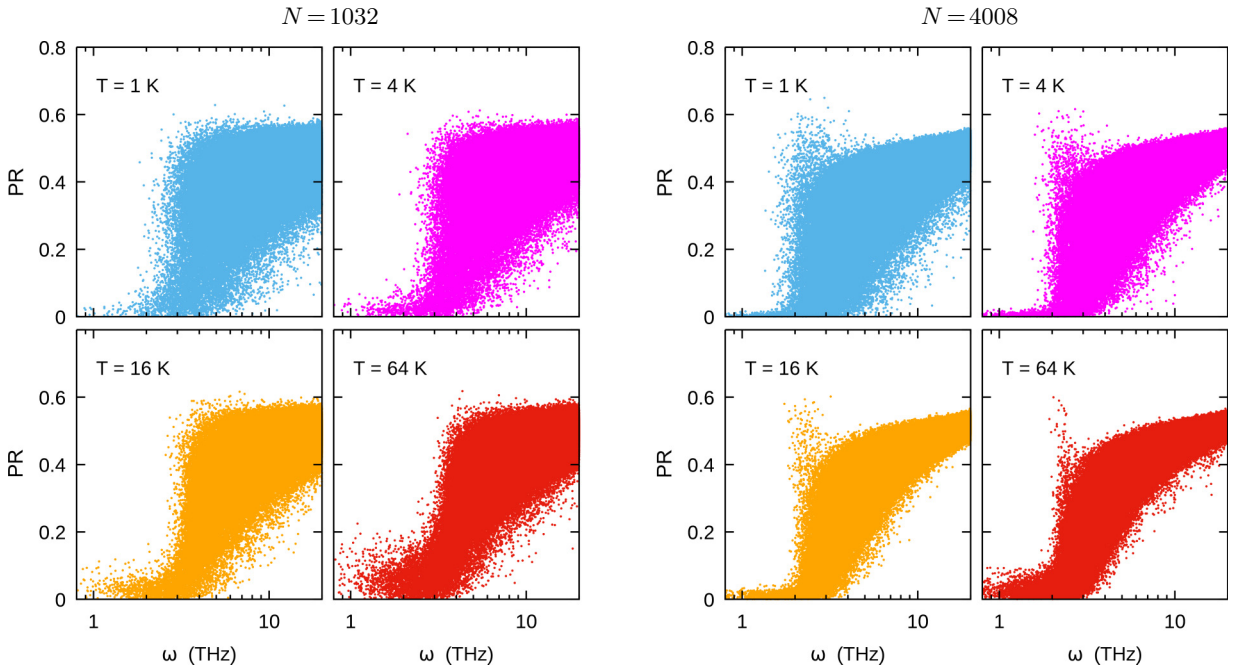

FIG. 3. Participation ratio [Eq. (3)] calculated for the (left panels) 1032-atoms and (right panels) 4008-atoms system at four different temperatures T.

II. THE MODEL SILICA GLASS

The silica glass is simulated in a three-dimensional cubic box for two different system sizes:

(1) $N = 1032$ atoms, therefore, $N_{\mathrm{Si}} = 344$ silicon atoms and $N_{\mathrm{O}} = 688$ oxygen atoms with a box length $L = 25$ Å.

(2) $N = 4008$ atoms, therefore, $N_{\mathrm{Si}} = 1336$ silicon atoms and $N_{\mathrm{O}} = 2672$ oxygen atoms with a box length $L = 39.3$ Å.

The interaction between atoms is given by Vashishta's potential [21]. In this paper, units are defined on the basis of energy, length, and time, respectively, being eV, angstroms, and picoseconds.

Preparation protocol. Following Ref. [4], glass samples are initially prepared with randomly positioned Si and O atoms with a density $\rho_{\mathrm{in}} = 2.196\ \mathrm{g/cm^3}$ and an annealing protocol: (i) 2 ps of Newtonian dynamics where atoms have Lennard-Jones interactions and are viscously damped with a rate of 1/ps and atomic velocities limited to 1 Å/ps, (ii) 8 ps of damped Newtonian dynamics with Vashishta's potential for silica glass. (iii) Heating up the system up to 4000 K and then quench to 0 K in 100 ps, corresponding to a cooling rate of 40 K/ps. The so-produced configurations are then minimized through the fast inertial relaxation engine [22] until the total force on every atom satisfies $|\boldsymbol{F}_i| \leqslant 10^{-10}$ eV/Å.

Simulations at nonvanishing temperatures. We perform simulations using a Langevin thermostat (damping parameter 1 ps) at $T = 1, 2, 4, 8$ K for 50 ps followed by microcanonical ensemble simulations for 100 ps (200 ps) for the smallest (largest) system size, monitoring the MSDs of the atoms. The total number of starting configurations for each temperature is 1000. Different from our previous works on silica glasses [23,24] where we used a different interatomic potential, we use here Vashishta's potential as implemented in LAMMPS [25] since it is more efficient in terms of computation time.

III. RESULTS

To guarantee that our measurements do not exceed the time window in which diffusion does not play a role, we measure the MSD of our atoms at each temperature T. Since the covariance matrix Eq. (6) has to be measured inside the glass basin, we must ensure that the system is still in the basin prepared at $t = 0$. Figure 1 presents the MSD as a function of time. Obviously, when the temperature is too high, the system escapes from the basin, preventing us from measuring a stationary covariance matrix. On the other hand for low temperatures (from $T = 1$ K up to $T = 32$ K), the MSD reaches a plateau which survives throughout our simulation window (1000 ps). Note that as the temperature increases, the plateau increases as expected from solid mechanics. At a finite temperature-dependent timescale τ_G the MSD departs from the plateau, meaning that diffusion sets in and the system departs from the local minimum. In practice, we have to compute the covariance matrix within the range of the plateau before the MSD displays the upturn.

We show the density of states obtained by the covariance matrix at finite temperatures (from 1 to 64 ;) in Fig. 2. Panels (a) and (b) show the density of states including all modes for the two system sizes, and the dashed lines correspond to the ω^4 scaling law. Only at very low frequency, the DOS appears to obey the ω^4 scaling; for $N = 1032$ the behavior is observed in a very short range of frequencies, but for the bigger sample $N = 4008$ this trend is clearer. To exhibit the scaling law more convincingly, we need to select only QLMs. To this end, we include only the modes having participation ratios below 0.1 (see Fig. 3). Indeed after these modes are selected, we see in panels (c) and (d) that the DOS obeys a clear ω^4 scaling. We note that in the case of the small system of 1032 atoms [Fig. 2(c)] at very low ω, the DOS is much smaller

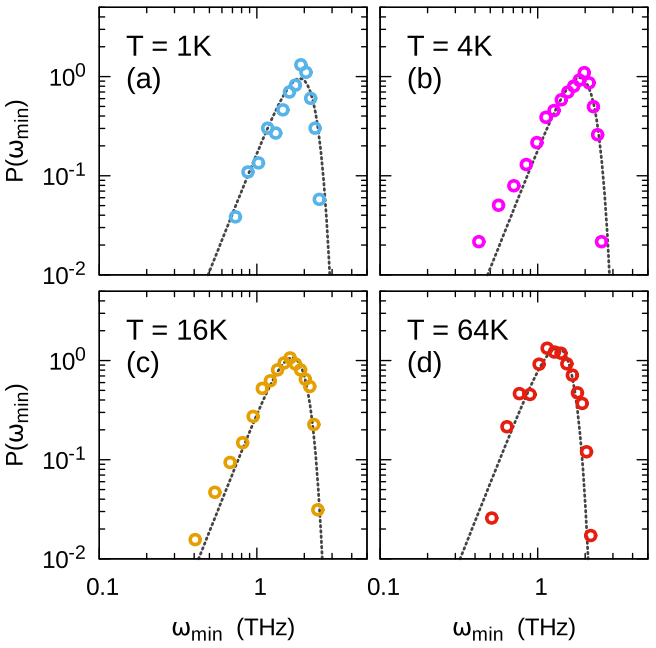

FIG. 4. Left panels: Distribution of the minimal vibrational frequency $P(\omega_{\min})$ for the largest investigated system size $N = 4008$ and four temperatures T. The dotted lines are the corresponding Weibull distributions, Eq. (12).

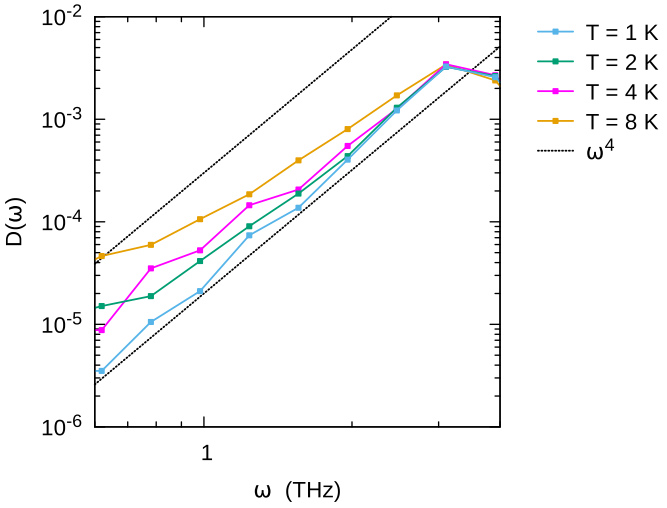

FIG. 5. Density of states as computed from the standard bare Hessian computed at the mean coordinates $\boldsymbol{R}_i$ at different temperatures $T = 1,\ 2,\ 4,$ and 8 K for SiO_2 glass samples of $N = 1032$ atoms. Only the modes with participation ratio smaller than 0.1 are considered. For all T values, statistics over 1000 samples was accounted.

than the expected ω^4 scaling; this is possibly due to finite size effects. Indeed in the larger samples of 4008 atoms in panel (d), the DOS shows ω^4 scaling down to the very lowest available frequencies. By fitting ω^p with the collapsed data of Figs. 2(c) and 4(d) in the 0.4-2.0-THz range we have obtained $p = 3.926 \pm 0.248$ and $p = 3.924 \pm 0.165$ for $N = 1032$ and $N = 4008$, respectively. The data shown in Fig. 2 indicates the presence of the ω^4 scaling law also at finite temperatures for the realistic silica glass model. Together with the previously investigated simple binary mixture systems [18], this implies that the ω^4 scaling law is robust and universal, existing in different glass models also at finite temperature.

It is interesting to note that recent analysis led two groups to present density of states with power laws following ω^3 [26] and ω^5 [27], respectively. Having in mind that in the present case the scaling range of the ω^4 scaling law is rather limited, we turn now to extreme value statistics to lend further support to the ω^4 law. Since we have many configurations in our simulations, we can determine the minimal frequency obtained from the diagonalization of $\mathbf{H}^{(\mathrm{eff})}$ in each and every configuration, denoting it as $\omega_{\min}$. The average of this minimal frequency over the ensemble of configurations is denoted $\langle\omega_{\min}\rangle$. Referring to the argument first presented in Ref. [28], we expect that in systems with N atoms,

$$\int_0^{\langle\omega_{\min}\rangle} D(\omega)d\omega \sim N^{-1}. \tag{10}$$

Using Eq. (4), we then expect that in three dimensions,

$$\langle\omega_{\min}\rangle \sim N^{-1/5} \sim L^{-3/5}. \tag{11}$$

Moreover, since the different realizations are uncorrelated, the values of $\omega_{\min}$ are also uncorrelated. Then the well-known Weibull theorem [29] predicts that the distribution of $\omega_{\min}$ should obey the Weibull distribution in the limit of large N,

$$W(\omega_{\min}) = \frac{5[\Gamma(1.2)]^5}{\langle\omega_{\min}\rangle^5}\,\omega_{\min}^4 \exp\left[-\left(\frac{\omega_{\min}\Gamma(1.2)}{\langle\omega_{\min}\rangle}\right)^5\right], \tag{12}$$

where $\Gamma(x)$ is the Γ function $\Gamma(1.2) \approx 0.918$. This prediction is tested in four left panels of Fig. 4. The distributions of $\omega_{\min}$ for four values of the temperature T are shown together with the predicted distributions as dictated by Eq. (12). We stress that there is no free fitting here, and, therefore, this is a strong independent test of Eq. (4). Note that the Weibull distribution is expected to apply only in the limit of large N. Indeed we found that our data for the smaller system with $N = 1032$ deviate from the predictions of Eq. (12).

IV. SUMMARY AND DISCUSSION

The main aim of this paper was to examine whether the universality class expressed by Eq. (4) extends to finite temperatures in glasses whose interactions are richer than those of simple glass formers with binary interactions [18]. One needs to understand that the bare Hessian, which can be computed for any snapshot of our thermal system, does not yield a scaling law of this form. This bare Hessian has, in principle, negative eigenvalues (i.e., imaginary frequencies) since any given state is unstable and is bound to evolve. In the case of our silica glass model, when computing the bare Hessian at the mean coordinates $\boldsymbol{R}_i$ of Eq. (5), very low temperature configurations do not have negative eigenvalues. But at higher temperatures the number of negative eigenvalues tends to increase rapidly with T; already at $T = 16$ K all the samples showed negative eigenvalues. Therefore, to consider the density of states one needs to exclude configurations with negative eigenvalues. Selecting these configurations only, and filtering according to the same criterion, i.e., including only

modes whose participation ratio is smaller than 0.1, we obtain the density of states shown in Fig. 5. The distribution resembles the unfiltered probability density functions in panels (a) and (b) of Fig. 2. To obtain probability density functions following the scaling law (4), we need to compute $\mathbf{H}^{(\mathrm{eff})}$ and filter out the modes with a high participation ratio.

ACKNOWLEDGMENTS

R.G. acknowledges financial support from Università degli Studi di Milano, Grant No. 1094 SEED 2020-TEQUAD. The work of I.P. was supported, in part, by the US-Israel Binational Science Foundation and the Minerva Foundation, Munich, Germany.

[1] W. Kob and H. C. Andersen, Kinetic lattice-gas model of cage effects in high-density liquids and a test of mode-coupling theory of the ideal-glass transition, Phys. Rev. E **48**, 4364 (1993).

[2] D. L. Malandro and D. J. Lacks, Relationships of shear-induced changes in the potential energy landscape to the mechanical properties of ductile glasses, J. Chem. Phys. **110**, 4593 (1999).

[3] C. E. Maloney and A. Lemaître, Amorphous systems in athermal, quasistatic shear, Phys. Rev. E **74**, 016118 (2006).

[4] S. Bonfanti, R. Guerra, C. Mondal, I. Procaccia, and S. Zapperi, Universal Low-Frequency Vibrational Modes in Silica Glasses, Phys. Rev. Lett. **125**, 085501 (2020).

[5] U. Buchenau, Y. M. Galperin, V. L. Gurevich, and H. R. Schober, Anharmonic potentials and vibrational localization in glasses, Phys. Rev. B **43**, 5039 (1991).

[6] V. Gurarie and J. T. Chalker, Bosonic excitations in random media, Phys. Rev. B **68**, 134207 (2003).

[7] V. L. Gurevich, D. A. Parshin, and H. R. Schober, Anharmonicity, vibrational instability, and the Boson peak in glasses, Phys. Rev. B **67**, 094203 (2003).

[8] D. A. Parshin, H. R. Schober, and V. L. Gurevich, Vibrational instability, two-level systems, and the boson peak in glasses, Phys. Rev. B **76**, 064206 (2007).

[9] E. Lerner, G. Düring, and E. Bouchbinder, Statistics and Properties of Low-Frequency Vibrational Modes in Structural Glasses, Phys. Rev. Lett. **117**, 035501 (2016).

[10] M. Baity-Jesi, V. Martín-Mayor, G. Parisi, and S. Perez-Gaviro, Soft Modes, Localization, and Two-Level Systems in Spin Glasses, Phys. Rev. Lett. **115**, 267205 (2015).

[11] L. Angelani, M. Paoluzzi, G. Parisi, and G. Ruocco, Probing the non-Debye low-frequency excitations in glasses through random pinning, Proc. Natl. Acad. Sci. USA **115**, 8700 (2018).

[12] M. Shimada, H. Mizuno, M. Wyart, and A. Ikeda, Spatial structure of quasilocalized vibrations in nearly jammed amorphous solids, Phys. Rev. E **98**, 060901(R) (2018).

[13] H. Mizuno, H. Shiba, and A. Ikeda, Continuum limit of the vibrational properties of amorphous solids, Proc. Natl. Acad. Sci. USA **114**, E9767 (2017).

[14] G. Kapteijns, E. Bouchbinder, and E. Lerner, Universal Nonphononic Density of States in 2D, 3D, and 4D Glasses, Phys. Rev. Lett. **121**, 055501 (2018).

[15] A. Moriel, G. Kapteijns, C. Rainone, J. Zylberg, E. Lerner, and E. Bouchbinder, Wave attenuation in glasses: Rayleigh and generalized-Rayleigh scattering scaling, J. Chem. Phys. **151**, 104503 (2019).

[16] D. Richard, K. González López G. Kapteijns, R. Pater, T. Vaknin, E. Bouchbinder, and E. Lerner, Universality of the Nonphononic Vibrational Spectrum across Different Classes of Computer Glasses, Phys. Rev. Lett. **125**, 085502 (2020).

[17] P. Das, V. Ilyin, and I. Procaccia, Instabilities of time-averaged configurations in thermal glasses, Phys. Rev. E **100**, 062103 (2019).

[18] P. Das and I. Procaccia, Universal Density of Low-Frequency States in Amorphous Solids at Finite Temperatures, Phys. Rev. Lett. **126**, 085502 (2021).

[19] O. Gendelman, E. Lerner, Y. G. Pollack, I. Procaccia, C. Rainone, and B. Riechers, Emergent interparticle interactions in thermal amorphous solids, Phys. Rev. E **94**, 051001(R) (2016).

[20] G. Parisi, I. Procaccia, C. Shor, and J. Zylberg, Effective forces in thermal amorphous solids with generic interactions, Phys. Rev. E **99**, 011001(R) (2019).

[21] J. Q. Broughton, C. A. Meli, P. Vashishta, and R. K. Kalia, Direct atomistic simulation of quartz crystal oscillators: Bulk properties and nanoscale devices, Phys. Rev. B **56**, 611 (1997).

[22] E. Bitzek, P. Koskinen, F. Gähler, M. Moseler, and P. Gumbsch, Structural Relaxation Made Simple, Phys. Rev. Lett. **97**, 170201 (2006).

[23] S. Bonfanti, E. E. Ferrero, A. L. Sellerio, R. Guerra, and S. Zapperi, Damage accumulation in silica glass nanofibers, Nano Lett. **18**, 4100 (2018).

[24] S. Bonfanti, R. Guerra, C. Mondal, I. Procaccia, and S. Zapperi, Elementary plastic events in amorphous silica, Phys. Rev. E **100**, 060602(R) (2019).

[25] A. P. Thompson, H. Metin Aktulga, R. Bergerc, D. S. Bolintineanu, W. Michael Brown, P. S. Crozier, P. J. in 't Veld, A. Kohlmeyer, S. G. Moore, T. DacNguyen *et al.*, LAMMPS - A flexible simulation tool for particle-based materials modeling at the atomic, meso, and continuum scales, Comp. Phys. Comm. **271**, 108171 (2022).

[26] L. Wang, G. Szamel, and E. Flenner, Low-Frequency Excess Vibrational Modes in Two-Dimensional Glasses, Phys. Rev. Lett. **127**, 248001 (2021).

[27] V. V. Krishnan, K. Ramola, and S. Karmakar, Universal non-Debye low-frequency vibrations in sheared amorphous solids, Soft Matter (2022).

[28] S. Karmakar, E. Lerner, and I. Procaccia, Phys. Rev. E **82**, 055103(R) (2010).

[29] W. Weibull, *A Statistical Theory of the Strength of Materials*, Ingeniörsvetenskapsakademuens Handlingar (Generalstabens litografiska anstalts förlag, Stockholm, 1939).